

# Enhanced pulse shaping filters for minimizing interference in GFDM signals for 5G cellular networks

Sairam Vamsi Tadikamalla<sup>1</sup>, Harish Chandra Mohanta<sup>2</sup>, Sudheer Kumar Terlapu<sup>3</sup>,  
Vamshi Krishna Mandhapati<sup>4</sup>

<sup>1</sup>Centurion University of Technology and Management, Odisha, India

<sup>2</sup>Department of Electronics and Communication Engineering, Centurion University of Technology and Management, Odisha, India

<sup>3</sup>Shri Vishnu Engineering College for Women, Bhimavaram, India

<sup>4</sup>Dhanekula Institute of Engineering and Technology, Vijayawada, India

## Article Info

### Article history:

Received Jul 8, 2024

Revised Oct 9, 2024

Accepted Nov 19, 2024

### Keywords:

GFDM

Modulation techniques

Pulse shaping filters

SER

## ABSTRACT

The imminent rise of 5th generation (5G) wireless standards heralds a pivotal era in cellular communication. Among the challenges faced, selecting an optimal multiple access technique stands out as crucial for achieving the desired blend of low latency, high data rates, and throughput. Generalized frequency division multiplexing (GFDM) emerges as a promising candidate meeting 5G requirements. This study introduces two innovative pulse shaping filters (PSFs) the better than raised cosine filter (BRFCF) and modified bartlett hanning filter (MBHF) paired with various modulation schemes such as binary phase shift keying (BPSK), quadrature phase shift keying (QPSK), and quadrature amplitude modulation (QAM) to assess GFDM signal performance. Considering its spectrum efficiency, QAM modulation emerges as the preferred choice. Performance evaluation of the PSFs entails analyzing symbol error rate (SER) against signal to noise ratio (SNR) across different modulation schemes.

*This is an open access article under the [CC BY-SA](#) license.*



## Corresponding Author:

Sairam Vamsi Tadikamalla  
Department of Electronics and Communication Engineering  
Centurion University of Technology and Management  
Odisha, India  
Email: vamsi.0438@gmail.com

## 1. INTRODUCTION

In recent years, significant transformations have occurred in both wired and wireless communication systems, largely driven by the dominance of digital technology. This shift has created a pressing demand for high data rates, increased throughput, and minimized latency [1]. Various sectors, including satellite and military applications, rely on exceptionally high data rates to support real-time connectivity among numerous devices [2]. Similarly, applications like vehicle automation necessitate minimal latency to swiftly execute operations, while banking systems require high throughput. Embracing the principles of Industry 4.0, which advocates for interconnected industries, mandates meeting these criteria [3]. The advent of 5th Generation (5G) wireless systems is poised to fulfill the demands of Industry 4.0 and global automation [4]. However, 5G technology must address specific requirements, including minimizing out-of-band (OOB) radiation and adjacent channel interference, reducing peak to average power ratio (PAPR), and enabling ultra-reliable, low-latency communication with an enhanced mobile broadband band [5].

In the realm of 5G technology, researchers face the challenge of achieving high data rates while minimizing interference, particularly in the context of multi-carrier modulation techniques [6]. Orthogonal frequency division multiplexing (OFDM), a well-known method employed in 4G and long-term evolution

(LTE) systems, exemplifies this [7]. OFDM's use of orthogonality and Cyclic Prefix (CP) enhances robustness and reduces frequency-selective fading compared to single-carrier techniques. However, OFDM has drawbacks such as high PAPR, inter-carrier interference (ICI), OOB emissions, and reliance on CP usage [8]. Consequently, OFDM has not been adopted for next-generation (5G) systems due to these limitations. The 5G now group is exploring four alternative waveforms for efficient air interface design, which do not rely on orthogonality and synchronization requirements [9]. These include filter bank multicarrier (FBMC), generalized frequency division multiplexing (GFDM), universal filtered multicarrier (UFMC), and Bi-orthogonal frequency division multiplexing (BFDM) [10]. Each of these techniques aims to reduce Inter-Symbol Interference (ISI) and increase spectral efficiency. However, GFDM stands out as the only multiplexing technique offering significantly low OOB radiation, addressing a crucial concern in 5G technology [11].

GFDM, a prominent multiplexing technique in the realm of 5G, represents the evolution of OFDM. Its key distinction from OFDM lies in the use of non-rectangular pulses instead of rectangular ones, eliminating the orthogonality characteristic. GFDM comprises multiple individual blocks, each modulated separately with multiple sub-carriers, and each subcarrier carrying various symbols [12]. Due to the absence of orthogonality, GFDM employs pulse shaping filters (PSFs) to mitigate interference. These PSFs play a crucial role in altering the characteristics of the modulated signal to be transmitted through the channel, essential for minimizing ISI caused by high modulation signals through band-limited channels [13]. While conventional filters like raised cosine filter (RCF) and root raised cosine filter (RRCF) are commonly applied in multiplexing schemes, they may not effectively reduce interference. This paper introduces novel PSFs such as better than raised cosine filter (BRCF) and modified bartlett hanning filter (MBHF), offering significant interference reduction compared to existing techniques [14].

The upcoming sections of the paper delve into the GFDM system model, accompanied by its performance analysis. This will be followed by a discussion on existing and proposed PSFs, along with a comparative analysis of results.

## 2. GFDM SYSTEM FRAMEWORK

GFDM employs non-orthogonal multicarrier modulation, transmitting information across  $K$  subcarriers and  $N$  sub-symbols. Unlike traditional methods, GFDM users operate within the same band and frequency simultaneously, with each user's information distinguished by power levels [15]. Consequently, GFDM demands substantial computational resources. Additionally, it leverages the superposition principle at the transmitter and implements successive interference cancellation at the receiver, allowing for the utilization of the same spectrum for all users. Figure 1 illustrates the block diagram of the GFDM model [16].

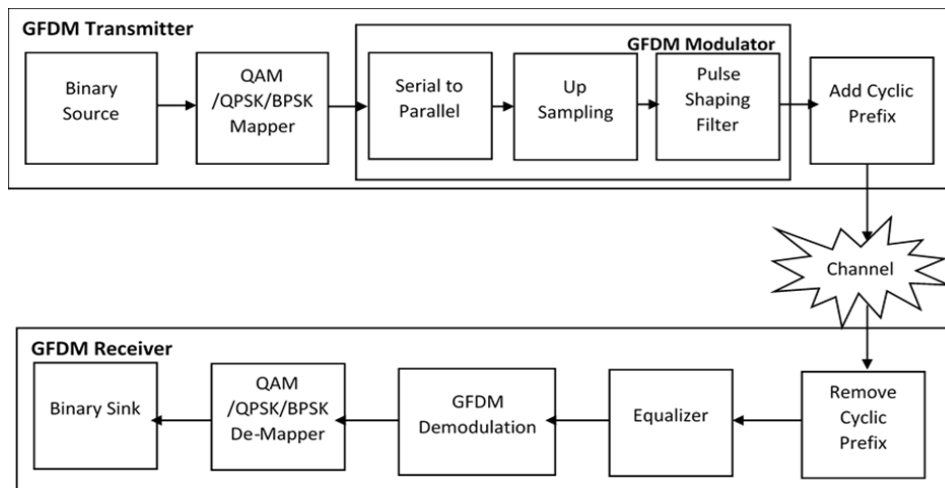


Figure 1. GFDM system model

In the transmitter part of GFDM, several operations are conducted including data generation, Mapping, GFDM modulation, and the addition of a CP. Con-stellation mapping is performed on binary data

to facilitate transmission over the channel. Among the three mappings available, quadrature amplitude modulation (QAM) mapper is commonly preferred for its ability to transmit two-bit streams or analog signals with varying amplitudes in a single transmission. At the receiver, these signals are separated and extracted to re-construct the original modulating signal [17]. The GFDM Modulator undertakes two primary operations: Up sampling and pulse shaping. Up sampling increases the modulation of the transmitted signal by padding zeros, maintaining the integrity of the content. Additionally, one of the PSFs is applied to generate the GFDM signal. CP is added to the GFDM signal to mitigate ISI during transmission through the channel. CP insertion involves appending the last  $M$  samples of the GFDM symbol to the front of the symbol [18].

This GFDM signal will be transmitted through the additive white gaussian noise (AWGN) channel and at receiver equalization is performed to recover transmitted symbols by reducing ISI [19].

#### - Calculation of SER for GFDM

In order to investigate the performance of different PSFs along with different modulations, it is necessary to generate GFDM matrix with the help of any PSFs. The previous section discusses different PSFs and they are indicated as  $P_{rcf}$ ,  $P_{brcf}$ , and  $P_{mbhf}$  and size of the filter is  $1 \times N_{SCM}$  [20]. The circular convolution has to be performed on the matrix obtained due to PSF in order to generate GFDM signal matrix of size  $N_{SCM} \times N_{SCM}$  and it is indicated as  $PC = \text{circshift}(P)$ , where  $P = P_{rcf}/P_{brcf}/P_{mbhf}$  and  $PC$  is the pulse shaping matrix after applying circular convolution [21]. In GFDM each symbol is the transmitter with a corresponding pulse shape which is written as,

$$x[k] = \sum_{n=0}^{N_{SC}-1} \sum_{m=0}^{M-1} d_{n,m} P_{n,m}[k] \quad (1)$$

where  $k = 0, 1, 2, \dots, N_{SC} M - 1$ ,  $d =$  Input binary sequence.

With the help of  $P_{n,m}[k]$  having matrix size  $1 \times N_{SCM}$  and  $PC$  having matrix size  $N_{SCM} \times 1$ , the GFDM matrix  $A$  formed and it can be written as,

$$x = Ad \quad (2)$$

where  $A$  is called as GFDM modulation matrix with size  $N_{SCM} \times N_{SCM}$ .

To analyse performance in terms of symbol error rate (SER) and signal to noise ratio (SNR) by assuming AWGN channel and it can be written as,

$$P_{AWGN} = 2 \left( \frac{v-1}{v} \right) \text{erfc}(\sqrt{\delta}) - \left( \frac{v-1}{v} \right)^2 \text{erfc}^2(\sqrt{\delta}) \quad (3)$$

$$\text{Where } \delta = \frac{3R_T}{2(2^\mu - 1)} \cdot \frac{E_s}{N_o} \quad (4)$$

$$\frac{E_s}{N_o} \text{ --- SNR in dB}$$

$$\text{and } R_T = \frac{N_{SC} \cdot M}{N_{SC} \cdot M + N_{CP} + N_{CS}} \quad (5)$$

$\mu$  is the number of bits per binary phase shift keying (BPSK)/quadrature phase shift keying (QPSK)/QAM symbol,  $v = \sqrt{2^\mu}$ ,  $N_{CP}$  and  $N_{CS}$  are the length of CP and Cyclic Suffix respectively,  $E_s$  is average energy per symbol,  $N_o$  is Noise power density.

Now the received signal  $y$  is formed by adding transmitted signal with noise.

$$y = x + P_{AWGN} \quad (6)$$

This signal has to be demodulated using transpose of GFDM transmitter matrix ( $A$ ) with the received signal after channel.

$$R_x = (A^T) * y \quad (7)$$

After demodulation, the analysis is conducted on the received signal to compare SER against SNR. Initially, SNR is assumed to be zero, with the size of the matrix equal to SNR in decibels. SER for each SNR is computed by measuring the difference in errors between the received and transmitted signals [22]. This can be expressed as (8).

$$[E_{err}, E_{avg}] = symerr(R_X, x) \quad (8)$$

The above will compare the elements in two matrices  $R_X$  and  $x$ . The number of differences is output in  $E_{err}$ . The ratio of  $E_{err}$  to the number of elements is output of  $E_{avg}$ . Now the SER will be calculated using.

$$\sum_{i=0}^{snr\_db} SER(i) = SER(i) + E_{avg} \quad (9)$$

In this paper, the  $snr\_db$  is taken from 0 to 20 db with 2 db interval.

### 3. ANALYSIS OF EXISTING PULSE SHAPING FILTER

These filters are integral to the generation of GFDM signals, as they modify the characteristics of the transmitted signal. The primary objective of employing PSFs is to optimize the transmitted signal for the channel conditions. Transmitting highly modulated signals in narrow bandwidth communication channels often results in ISI. PSFs are utilized to mitigate ISI by narrowing the bandwidth of the modulated signal in accordance with the channel characteristics, thereby influencing the overall properties of the GFDM signal [23].

- Raised cosine filter

Unlike the constraints associated with using rectangular pulses in OFDM, the RCF adopts the fourier transform of a rectangular pulse, namely the sinc pulse. This choice is particularly advantageous for band-limited data transmission, as it offers superior suitability and performance [24].

Let  $P_{ref}(\omega)$  be the spectrum of RCF and  $\gamma$  will be rolling factor then spectrum for RCF is existed in between.

$$P_{ref}(\omega) = \tau \text{ for } 0 \leq \omega \leq \frac{\pi(1-\gamma)}{\tau} \quad (10)$$

$$P_{ref}(\omega) = \frac{\tau}{2} \left( 1 - \sin \left( \left( \frac{\tau}{2\gamma} \right) \left( \omega - \frac{\pi}{\tau} \right) \right) \right) \text{ for } \frac{\pi(1-\gamma)}{\tau} \leq \omega \leq \frac{\pi(1+\gamma)}{\tau} \quad (11)$$

$$P_{ref}(\omega) = 0 \text{ for } \omega \geq \frac{\pi(1+\gamma)}{\tau} \quad (12)$$

$P_{ref}(\omega)$  forms a sinc pulse which is existed in between  $\frac{\pi(1-\gamma)}{\tau} \leq \omega \leq \frac{\pi(1+\gamma)}{\tau}$  and no pulse is existed after  $\omega \geq \frac{\pi(1+\gamma)}{\tau}$ , due to this nature ISI can be reduced.

The time response of  $P_{ref}(t)$  is obtained by applying inverse fourier transform to  $P_{ref}(\omega)$ . The response signal of RCF is taken by combining two signals which are  $90^\circ$  phases to each other. Those signals are:

$$P_{ref1}(t) = \sin \left( \frac{\pi t}{T} (1 - \gamma) \right) \text{ and } P_{ref2}(t) = \cos \left( \frac{\pi t}{T} (1 + \gamma) \right) \text{ then}$$

$$P_{ref}(t) = \frac{P_{ref1}(t) + \frac{4\gamma t}{T} P_{ref2}(t)}{\frac{\pi t}{T} \left( 1 - \left( \frac{4\gamma t}{T} \right)^2 \right)} \quad (13)$$

where  $\gamma$  is roll off factor, the response of GFDM signal is varied by varying  $\gamma$  in between 0 to 1 and  $T$  is the symbol period [25].

### 4. ANALYSIS OF PROPOSED PULSE SHAPING FILTERS

The existing filter consists of only one variable parameter such as roll off factor ( $\gamma$ ). Along with  $\gamma$ , the proposed filters consist of sensitivity variable and windowing variable. Due to these additional variable parameters, the shape of the pulse is varied such that interference decreases.

#### 4.1. Better than raised cosine filter

This filter gives better pulse shaping compared to RCF by introducing sensitivity variable named as  $\beta$  [26]. The response of this filter is given by (14).

$$P_{\text{brcf1}}(t) = \sin\left(\frac{\pi\gamma\tau}{T}\right) \text{ and } P_{\text{brcf2}}(t) = \cos\left(\frac{\pi\gamma\tau}{T}\right)$$

$$P_{\text{brcf}}(t) = \text{sinc}\left(\frac{\tau}{T}\right) \frac{2\beta\tau/T P_{\text{brcf1}}(t) + 2 P_{\text{brcf2}}(t) - 1}{1 + (\beta\tau/T)^2} \quad (14)$$

where  $T$  is the transmission period and  $\beta = \ln(2)/\gamma T$ .

#### 4.2. Modified bartlett hanning filter

This filter introduces a window shaping parameter denoted as  $\alpha$ , typically ranging between 0.5 to 1.88. Remarkably, this parameterization yields superior shaping compared to other filters [27]. The response of this filter is characterized by (15).

$$P_{\text{mbhf1}}(t) = \sin\left(\frac{\pi\alpha\tau}{T}\right) \text{ and } P_{\text{mbhf2}}(t) = \cos\left(\frac{\pi\alpha\tau}{T}\right)$$

$$P_{\text{mbhf}}(t) = \text{sinc}\left(\frac{\tau}{T}\right) \left[ \left( \frac{2(1-\alpha) P_{\text{mbhf1}}(t)}{1 - \left(\frac{2\gamma\tau}{T}\right)^2} \right) - \left( \frac{(1-2\alpha) P_{\text{mbhf1}}(t)}{\left(\frac{\gamma\tau}{T}\right)} \right) \right] \quad (15)$$

There are different pulse shapes are formed by varying  $\alpha$  and  $\gamma$  parameters. The Table 1 shows those types of filters.

Table 1. Different PSFs based on  $\alpha$  and  $\gamma$  parameters

$\alpha$	$\gamma$	Type of filter
0.5 to 1.88	0	Rectangular pulse shape filter
0.5	0 to 1	Raised cosine pulse shape filter
1	0 to 1	Bartlett hanning filter
1	1	Frank pulse shaping filter

From the Table 1, when windowing parameter  $\gamma$  is 0, then type of filter is rectangular pulse shape filter which is generally used for OFDM modulation techniques [28].

## 5. RESULTS AND DISCUSSION

In this section, a comparison is conducted among all three PSFs by varying the roll-off factor as 0.1, 0.5, and 0.9. The chosen modulation technique is QAM, as it consistently yields superior results compared to the other modulation techniques. The simulation environment for this analysis is outlined in Table 2.

Throughout the entire analysis, the roll-off factor is varied as 0.1, 0.5, and 0.9. Typically, the roll-off factor ranges from 0 to 1, and as it increases from 0 to 1, interference also increases, consequently leading to higher SER values. Therefore, to facilitate a clear understanding, values are chosen at the initial (0.1), middle (0.5), and end (0.9) of this range.

Table 2. Simulation environment considered for analysis

Parameter	Preferred value
No. of sub carriers	64
Sub symbols per block	6
Cyclic prefix length	16
No of bits per symbol	3
Modulation technique	BPSK, QPSK, QAM
PSF	RCF, BRCF, MBHF
SNR (in dB)	0, 2, 4, ..., 20
Roll off factor	0.1, 0.5, and 0.9
Window shaping parameter (used only for MBHF)	0.5 to 1.88

Upon examination of Figures 2-4, along with Table 3, it becomes apparent that the SER is impacted by an increase in the roll-off factor. Specifically, as the roll-off factor increases, it takes a longer time to achieve significantly low SER values relative to SNR. Furthermore, it is observed that the MBHF consistently yields very low SER values in comparison to the other two PSFs. Additionally, MBHF demonstrates superior linearity characteristics when compared to the remaining filters.

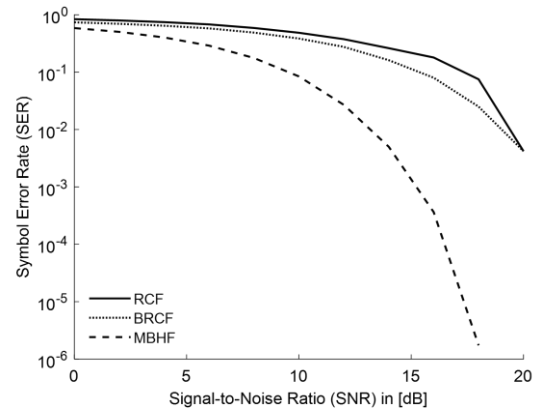
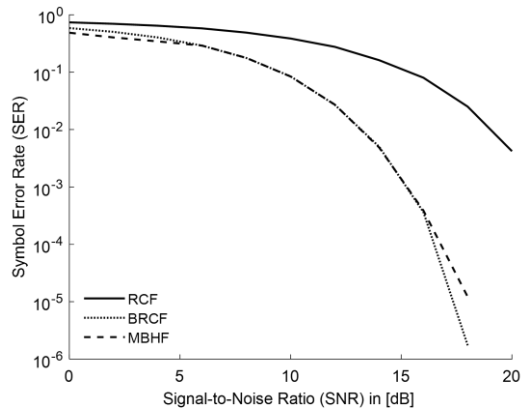


Figure 2. SER vs SNR plot with roll off factor 0.1      Figure 3. SER vs SNR plot with roll off factor 0.5

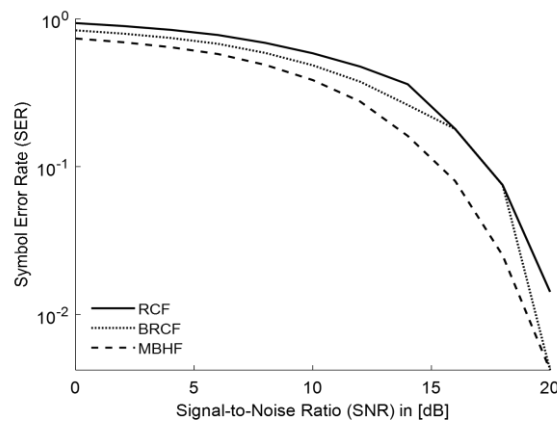


Figure 4. SER vs SNR plot with roll off factor 0.9

Table 3. Comparative analysis of existing and proposed filters

0	2	4	6	8	10	12	14	16	18	20	Modulation	Roll off	PSF
0.74	0.7	0.64	0.58	0.49	0.39	0.28	0.16	0.08	0.03	0	QAM	0.1	RCF
0.59	0.5	0.4	0.29	0.18	0.08	0.03	0.01	0	0	0			BRCF
0.49	0.4	0.34	0.29	0.18	0.08	0.03	0	0	0	0			MBHF
0.84	0.8	0.74	0.68	0.59	0.49	0.38	0.26	0.18	0.08	0		0.5	RCF
0.74	0.7	0.64	0.58	0.49	0.39	0.28	0.16	0.08	0.03	0			BRCF
0.59	0.5	0.4	0.29	0.18	0.08	0.03	0.01	0	0	0			MBHF
0.94	0.9	0.84	0.78	0.69	0.59	0.48	0.36	0.18	0.08	0.01		0.9	RCF
0.84	0.8	0.74	0.68	0.59	0.49	0.38	0.26	0.18	0.08	0			BRCF
0.74	0.69	0.64	0.58	0.49	0.38	0.27	0.16	0.08	0.02	0			MBHF

### 5.1. Modified bartlett hanning filter

In this section the analysis is done by taking individual filter with all three modulation techniques and roll off factors. Figure 5 specifies different types of pulse-shaping filters, along with modulation techniques, by varying the roll-off factors for different filters used in the analysis presented in this paper.

#### 5.1.1. Raised cosine filter

This section introduces the fundamental PSF utilized for generating GFDM signals. The characteristics of the SER vs SNR plot are observed to vary by altering the roll-off factor within the range of 0 to 1. Specifically, roll-off factors of 0.1, 0.5, and 0.9 are selected, alongside varying types of modulation techniques.

Based on Figures 6-8, as well as Table 4, the SER vs SNR plots for GFDM using three different modulations and varying roll-off factors of 0.1, 0.5, and 0.9 are pre-sented, employing the RCF filter. From the plots, it is evident that BPSK modulation yields superior SER values, with the SER reaching its minimum within a 10 dB SNR range.

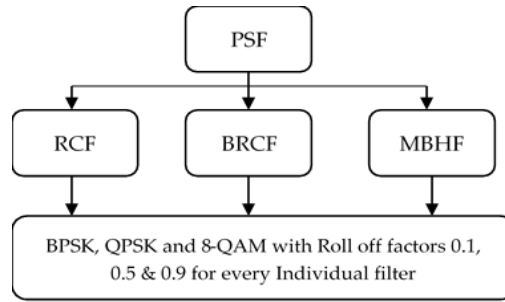


Figure 5. Types of PSFs

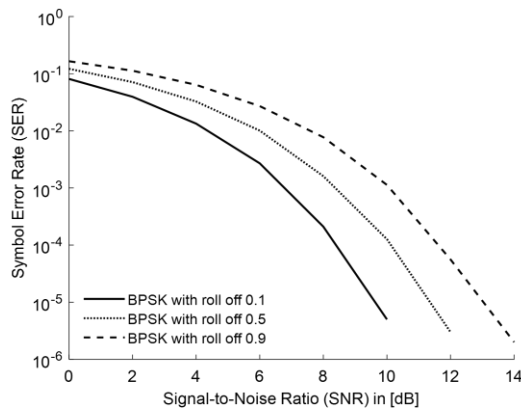


Figure 6. SER vs SNR plot of RCF with BPSK

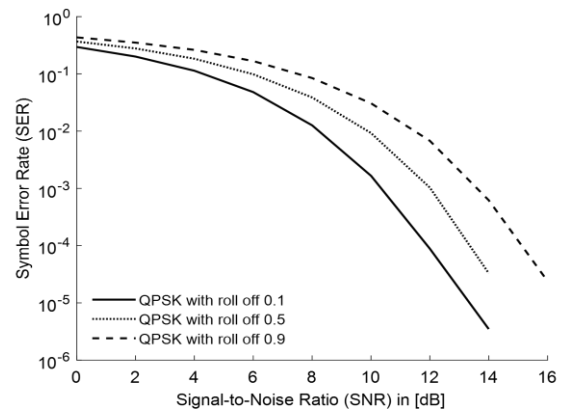


Figure 7. SER vs SNR plot of RCF with QPSK

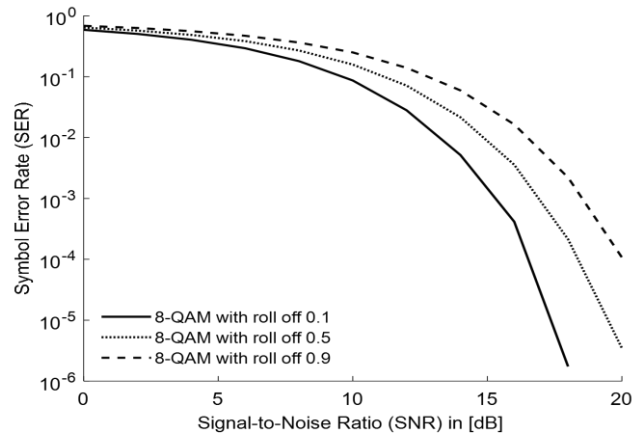


Figure 8. SER vs SNR plot of RCF with 8-QAM

Table 4. Comparative analysis of RCF with three modulations

0	2	4	6	8	10	12	14	16	18	20	Modulation	Roll off
0.08	0.04	0.01	0	0	0	0	0	0	0	0	BPSK	0.1
0.12	0.07	0.03	0.01	0	0	0	0	0	0	0	BPSK	0.5
0.17	0.11	0.06	0.03	0.01	0	0	0	0	0	0	BPSK	0.9
0.3	0.2	0.11	0.05	0.01	0	0	0	0	0	0	QPSK	0.1
0.37	0.28	0.18	0.1	0.04	0.01	0	0	0	0	0	QPSK	0.5
0.43	0.35	0.26	0.17	0.08	0.03	0.01	0	0	0	0	QPSK	0.9
0.59	0.51	0.41	0.29	0.18	0.09	0.03	0.01	0	0	0	QAM	0.1
0.64	0.57	0.49	0.38	0.27	0.16	0.07	0.02	0	0	0	QAM	0.5

### 5.1.2. Better than raised cosine filter

The sensitivity variable has been introduced in BRCF to produce better SER vs SNR plots compared to RCF. Here also BRCF is applied by changing type of modulations.

Based on Figures 9-11, as well as Table 5, the analysis of the BRCF filter with three different modulations is presented. Upon observation, it is noted that BPSK modulation exhibits superior characteristic curves compared to QAM and QPSK, as it yields significantly lower SER values and reaches the minimum within a 10 dB SNR range. Furthermore, in comparison to the characteristics of the RCF filter, the curves produced by the BRCF filter demonstrate better linearity in terms of SER values.

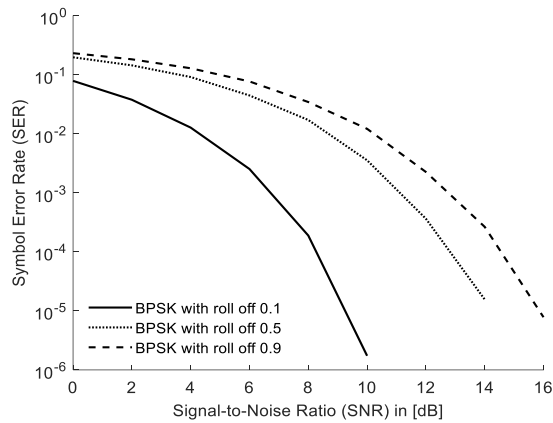


Figure 9. SER vs SNR plot of BRCF with BPSK

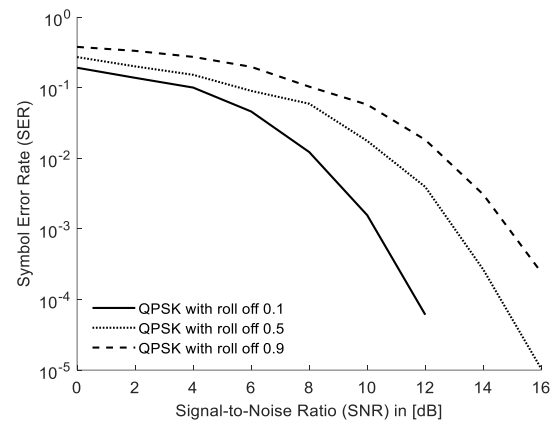


Figure 10. SER vs SNR plot of BRCF with QPSK

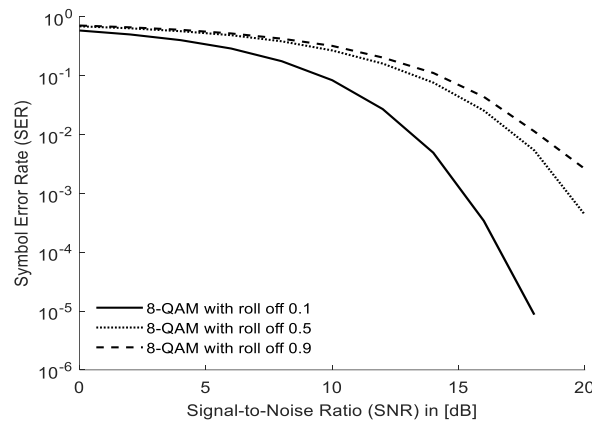


Figure 11. SER vs SNR plot of BRCF with 8-QAM

Table 5. Comparative analysis of BRCF with three modulations

0	2	4	6	8	10	12	14	16	18	20	Modulation	Roll off
0.08	0.04	0.01	0	0	0	0	0	0	0	0	BPSK	0.1
0.2	0.14	0.09	0.04	0.02	0	0	0	0	0	0	BPSK	0.5
0.23	0.18	0.13	0.08	0.03	0.01	0	0	0	0	0	BPSK	0.9
0.19	0.14	0.1	0.05	0.01	0	0	0	0	0	0	QPSK	0.1
0.27	0.2	0.15	0.09	0.06	0.02	0	0	0	0	0	QPSK	0.5
0.38	0.33	0.27	0.2	0.1	0.06	0.02	0	0	0	0	QPSK	0.9
0.59	0.5	0.4	0.29	0.18	0.08	0.03	0	0	0	0	QAM	0.1
0.69	0.64	0.57	0.49	0.38	0.27	0.16	0.08	0.03	0.01	0	QAM	0.5

### 5.1.3. Modified bartlett hanning filter

This MBHF introduces Windowing parameter ( $\alpha$ ) to increase characteristics of GFDM SER vs SNR performance. In general, the Windowing parameter is considered as 1 for all three modulations. From Figures 12-14, along with Table 6, the analysis of MBHF with three different modulations is presented. Upon



observation, it is evident that QAM modulation exhibits significantly lower SER values, with its value decreasing to very low levels within a 10 dB SNR range.

Upon comparing all three PSFs with three modulation techniques, it is evident that QAM modulation with the MBHF yields favourable SER vs SNR plots for GFDM signals. This paper comprehensively examines all curves while employing 8-QAM modulation, and it is noted that increasing the size of QAM may lead to even better performance results.

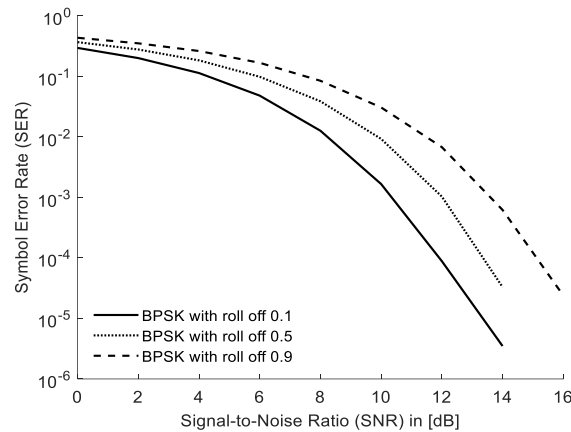


Figure 12. SER vs SNR plot of MBHF with BPSK

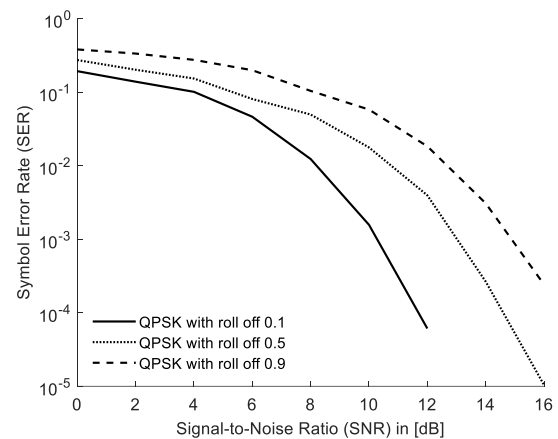


Figure 13. SER vs SNR plot of MBHF with QPSK

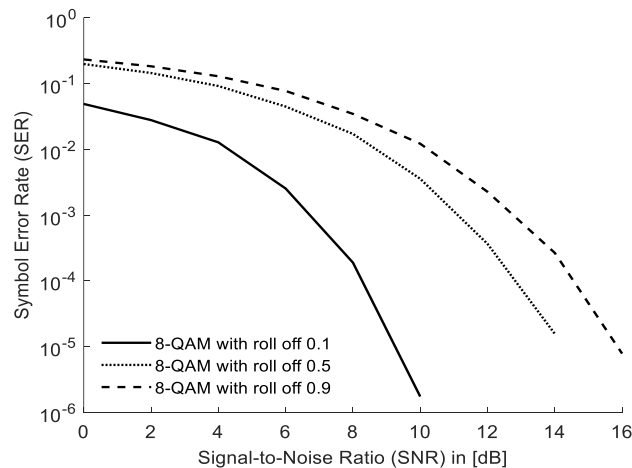


Figure 14. SER vs SNR plot of MBHF with 8-QAM

Table 6. Comparative analysis of MBHF with three modulations

0	2	4	6	8	10	12	14	16	18	20	Modulation	Roll off
0.08	0.04	0.01	0	0	0	0	0	0	0	0	BPSK	0.1
0.2	0.14	0.09	0.04	0.02	0	0	0	0	0	0	BPSK	0.5
0.23	0.18	0.13	0.08	0.03	0.01	0	0	0	0	0	BPSK	0.9
0.19	0.14	0.1	0.05	0.01	0	0	0	0	0	0	QPSK	0.1
0.27	0.2	0.15	0.09	0.06	0.02	0	0	0	0	0	QPSK	0.5
0.38	0.33	0.27	0.2	0.1	0.06	0.02	0	0	0	0	QPSK	0.9
0.59	0.5	0.4	0.29	0.18	0.08	0.03	0	0	0	0	QAM	0.1
0.69	0.64	0.57	0.49	0.38	0.27	0.16	0.08	0.03	0.01	0	QAM	0.5

## 6. CONCLUSION

The SER has been analysed as a function of SNR for various PSFs using modulation schemes BPSK, QPSK, and QAM. The results clearly demonstrate that the proposed filters, BRCF and MBHF, coupled with QAM modulation, exhibit superior performance in terms of SER against SNR compared to the

existing RCF filter. Additionally, the roll-off factor is examined for all modulation schemes across the three filters, revealing that the amplitude of the signal generated with the GFDM scheme decreases while the SER increases with an increase in the roll-off factor.





## REFERENCES

- [1] S. P. Bendale and J. Rajesh Prasad, "Security threats and challenges in future mobile wireless networks," in *Proceedings - 2018 IEEE Global Conference on Wireless Computing and Networking, GCWCN 2018*, Nov. 2018, pp. 146–150, doi: 10.1109/GCWCN.2018.8668635.
- [2] A. Khalid, "The concept of fifth generation (5G) mobile technology," *Communications on Applied Electronics*, vol. 2, no. 8, pp. 45–48, Sep. 2015, doi: 10.5120/cae2015651853.
- [3] Z. Wei *et al.*, "Orthogonal time-frequency space modulation: a promising next-generation waveform," *IEEE Wireless Communications*, vol. 28, no. 4, pp. 136–144, Aug. 2021, doi: 10.1109/MWC.001.2000408.
- [4] S. P. Sotiroudis, G. Athanasiadou, G. Tsoulos, P. Sarigiannidis, C. G. Christodoulou, and S. K. Goudos, "Evolutionary ensemble learning pathloss prediction for 4G and 5G flying base stations with UAVs," *IEEE Transactions on Antennas and Propagation*, vol. 71, no. 7, pp. 5994–6005, Jul. 2023, doi: 10.1109/TAP.2023.3266784.
- [5] M. Hu, J. Wang, W. Cheng, and H. Zhang, "Near-optimal piecewise linear companding transform for PAPR reduction of OFDM systems," *IEEE Transactions on Broadcasting*, pp. 1–10, 2024, doi: 10.1109/tbc.2024.3443466.
- [6] H. J. Taha and M. F. M. Salleh, "Multi-carrier transmission techniques for wireless communication systems: a survey," *WSEAS Transactions on Communications*, vol. 8, no. 5, pp. 457–472, 2009.
- [7] W. Jiang, X. Kuai, X. Yuan, W. Liu, and Z. Song, "Sparsity-learning-based iterative compensation for filtered-OFDM with clipping," *IEEE Communications Letters*, vol. 24, no. 11, pp. 2483–2487, Nov. 2020, doi: 10.1109/LCOMM.2020.3011680.
- [8] S. Jang, D. Na, and K. Choi, "Comprehensive performance comparison between OFDM-based and FBMC-based uplink systems," in *International Conference on Information Networking*, Jan. 2020, vol. 2020-January, pp. 288–292, doi: 10.1109/ICOIN48656.2020.9016425.
- [9] T. S. Vamsi, S. K. Terlapu, and M. V. Krishna, "Investigation of channel estimation techniques using OFDM with BPSK QPSK and QAM modulations," in *Proceedings - 2022 International Conference on Computing, Communication and Power Technology, IC3P 2022*, Jan. 2022, pp. 209–213, doi: 10.1109/IC3P52835.2022.00051.
- [10] K. Kiruthiga and N. R. Nagarajan, "An ease UFMC transmitter using IFFT," in *2019 International Conference on Intelligent Computing and Control Systems, ICCS 2019*, May 2019, pp. 1–5, doi: 10.1109/ICCS45141.2019.9065779.
- [11] S. Kalsotra, A. Kumar, H. D. Joshi, A. K. Singh, K. Dev, and M. Magarini, "Impact of pulse shaping design on OOB emission and error probability of GFDM," in *IEEE 5G World Forum, 5GWF 2019 - Conference Proceedings*, Sep. 2019, pp. 226–231, doi: 10.1109/5GWF.2019.8911699.
- [12] N. Michailow *et al.*, "Generalized frequency division multiplexing for 5th generation cellular networks," *IEEE Transactions on Communications*, vol. 62, no. 9, pp. 3045–3061, Sep. 2014, doi: 10.1109/TCOMM.2014.2345566.
- [13] J. Wu, X. Ma, X. Qi, Z. Babar, and W. Zheng, "Influence of pulse shaping filters on PAPR performance of underwater 5G communication system technique: GFDM," *Wireless Communications and Mobile Computing*, vol. 2017, pp. 1–7, 2017, doi: 10.1155/2017/4361589.
- [14] N. C. Beaulieu and M. O. Damen, "Parametric construction of Nyquist-I pulses," *IEEE Transactions on Communications*, vol. 52, no. 12, pp. 2134–2142, Dec. 2004, doi: 10.1109/TCOMM.2004.838739.
- [15] A. Lizeaga, P. M. Rodríguez, I. Val, and M. Mendicute, "Evaluation of 5G modulation candidates WCP-COQAM, GFDM-OQAM, and FBMC-OQAM in low-band highly dispersive wireless channels," *Journal of Computer Networks and Communications*, vol. 2017, pp. 1–11, 2017, doi: 10.1155/2017/2398701.
- [16] C. Sharma, S. K. Tomar, and A. Kumar, "A comparison of GFDM and OFDM at same and different spectral efficiency condition," in *Lecture Notes on Data Engineering and Communications Technologies*, vol. 33, 2020, pp. 282–293.
- [17] M. Maraş, E. N. Ayvaz, M. Gömeç, A. Savaşçıbaşı, and A. Özen, "A novel gfdm waveform design based on cascaded wht-lwt transform for the beyond 5g wireless communications," *Sensors*, vol. 21, no. 5, pp. 1–20, Mar. 2021, doi: 10.3390/s21051831.
- [18] M. Sheikh-Hosseini and S. Ahmadi, "Performance analysis of OFDM and GFDM techniques over additive white impulsive noise channels," in *Conference on Millimeter-Wave and Terahertz Technologies, MMWaTT*, Dec. 2022, vol. 2022-December, pp. 1–5, doi: 10.1109/MMWaTT58022.2022.10172127.
- [19] P. Wei, Y. Xiao, L. Dan, L. Ge, and W. Xiang, "N-continuous signaling for GFDM," *IEEE Transactions on Communications*, vol. 68, no. 2, pp. 947–958, Feb. 2020, doi: 10.1109/TCOMM.2019.2952601.
- [20] A. Kumar and M. Magarini, "Improved Nyquist pulse shaping filters for generalized frequency division multiplexing," in *2016 8th IEEE Latin-American Conference on Communications, LATINCOM 2016*, Nov. 2016, pp. 1–7, doi: 10.1109/LATINCOM.2016.7811588.
- [21] S. K. Bandari, V. V. Mani, and A. Drosopoulos, "Multi-taper implementation of GFDM," in *IEEE Wireless Communications and Networking Conference, WCNC*, Apr. 2016, pp. 1–5, doi: 10.1109/WCNC.2016.7564952.
- [22] T. Sairam Vamsi, S. K. Terlapu, and M. Vamsi Krishna, "PAPR Analysis of FBMC and UFMC for 5G cellular communications," in *Smart Innovation, Systems and Technologies*, vol. 266, 2022, pp. 351–358.
- [23] E. N. O. Herawati, A. F. Isnawati, and K. Niamah, "Analysis of GFDM-OQAM performance using zero forcing equalization," in *10th IEEE International Conference on Communication, Networks and Satellite, Comnetsat 2021 - Proceedings*, Jul. 2021, pp. 135–140, doi: 10.1109/COMNETSAT53002.2021.9530809.
- [24] K. Gentile, "The care and feeding of digital pulse-shaping filters," *RF Design*, vol. 25, no. 4, pp. 50–59, 2002.
- [25] H. M. Abdel-Atty, W. A. Raslan, and A. T. Khalil, "Evaluation and analysis of FBMC/OQAM systems based on pulse shaping filters," *IEEE Access*, vol. 8, pp. 55750–55772, 2020, doi: 10.1109/ACCESS.2020.2981744.
- [26] N. C. Beaulieu, C. C. Tan, and M. O. Damen, "A 'better than' Nyquist pulse," *IEEE Communications Letters*, vol. 5, no. 9, pp. 367–368, Sep. 2001, doi: 10.1109/4234.951379.





- [27] R. Saxena and H. D. Joshi, "Performance improvement in an OFDM system with MBH combinational pulse shape," *Digital Signal Processing: A Review Journal*, vol. 23, no. 1, pp. 314–321, Jan. 2013, doi: 10.1016/j.dsp.2012.09.010.
- [28] M. Kaur, H. D. Joshi, A. kumar, and M. Magarini, "DGT-based pulse shaping filter for generalized frequency division multiplexing system," *Physical Communication*, vol. 61, p. 102227, Dec. 2023, doi: 10.1016/j.phycom.2023.102227.

## BIOGRAPHIES OF AUTHORS







**Sairam Vamsi Tadikamalla**     is a research scholar at Centurion University of Technology and Management, currently working as an embedded software engineer at Bitsilica since 2023. With a total of 8 years of teaching experience, Vamsi has contributed significantly to the academic community by publishing 6 international journal papers and 10 international conference papers. Their areas of expertise are embedded and communication engineering. He can contact at email of vamsi.0438@gmail.com.







**Dr. Harish Chandra Mohanta**     holds an M.Tech. in Electronics and Communication Engineering from IIT Kharagpur and a Ph.D. in Electrical and Electronics Engineering from Deakin University, Australia. He has excelled in national level exams like GATE and UGC-NET and has developed significant expertise in antenna design. His doctoral research focused on developing a miniaturized rectenna for wireless power and energy harvesting. With over 16 years of teaching experience, he has published 38 research papers, authored 5 books, and secured 8 patents. Dr. Mohanta supervises multiple Ph.D. students and leads the ECE department at Centurion University of Technology and Management. He is also the CEO of the smart engineering applications research center and director of miniaturized solutions and applications private limited. He can be contacted at email: harishmohanta@cutm.ac.in.



**Dr. Sudheer Kumar Terlapu**     holds a B.E in Electronics and Communication Engineering and an M.Tech in Radar and Microwave Engineering from Andhra University, where he also earned his Ph.D. in Antenna Array Optimization and Pattern Synthesis. With 18 years of teaching and research experience, he is currently an Associate Professor in ECE at Shri Vishnu Engineering College for Women. He has published 51 research articles and is a Senior Member of IEEE, Fellow of IETE, and member of various professional societies. Dr. Sudheer has served on multiple academic and executive committees, including IEEE and IETE. He is an active reviewer for several journals and has chaired sessions at international conferences. His research interests include signal processing and antenna array optimization. He has guided two Ph.D. scholars and is currently supervising five. Dr. Sudheer has received awards for his contributions to pedagogical innovation and educational leadership. He can be contacted at email: profsudheer@ieee.org.



**Dr. Vamshi Krishna Mandhapati**     is a Professor and Head of Department in the Department of Electronics and Communication Engineering at Dhanekula Institute of Engineering and Technology, where he has been serving since October 19, 2020. With 13 years of experience, including 11 years in teaching and 2 years in research, Dr. Vamshi Krishna specializes in Radar and Microwave Engineering. He holds an Ph.D. in Computational electromagnetics and antennas from Centurion University, Odisha, M.Tech. in Radar and Microwave from Andhra University, Visakhapatnam, and a B.Tech. in Electronics and Communication Engineering from JITM under Biju Patnaik University of Technology (BPUT). His research interests include applied electromagnetics, antenna design, and wireless communication. Throughout his career, he has contributed significantly to his field, with a total of 45 publications in both international journals and conferences. He can be contacted at email: vamshi51@yahoo.co.in.